Supporting Information

Lewis acid-triggered photocatalytic hydrogen peroxide production in an aluminum-based metal-organic framework

Yoshifumi Kondo,[a] *Kenta Hino,*[a] *Yasutaka Kuwahara,*[a,b,c] *Kohsuke Mori,*[a,b] *Hisayoshi Kobayashi*,[a] *and Hiromi Yamashita**[a,b]

[a] Division of Materials and Manufacturing Science, Graduate School of Engineering, Osaka University, 2-1 Yamadaoka, Suita, Osaka 565-0871, Japan.
[b] Innovative Catalysis Science Division, Institute for Open and Transdisciplinary Research Initiatives (OTRI), Osaka University, 2-1 Yamadaoka, Suita, Osaka 565-0871, Japan.
[c] JST, PRESTO, 4-1-8 Honcho, Kawaguchi, Saitama 332-0012, Japan.

Table of contents

Experimental Section

Materials

Aluminum chloride hexahydrate ($AlCl_3 \cdot 6H_2O$), chromium nitrate nonahydrate ($Cr(NO_3)_3 \cdot 9H_2O$), iron chloride hexahydrate ($FeCl_3 \cdot 6H_2O$), *N,N*-dimethylformaldehyde (DMF), methanol, acetone, dichloromethane, pyridine, sodium hydroxide (NaOH), benzyl alcohol, hydrogen peroxide (H_2O_2), hydrochloric acid (HCl) and perchloric acid ($HClO_4$) were purchased from Nacalai Tesque. 2-aminoterephthalic acid, 2-nitroterephthalic acid, *tert*-butyl nitrite (*t*-BuONO), deuterium oxide (D_2O), Oxo[5,10,15,20-tetra(4-pyridyl)porphinato]titanium(IV) ($TiO(tpypH_4)^{4+}$) and 5,5-dimethyl-1-pyrroline *N*-oxide (DMPO) were purchased from Tokyo Chemical Industry Co., Ltd.. Hydrogen fluoride (HF) was purchased from FUJIFILM Wako Pure Chemical Corporation. Tin chloride dihydrate ($SnCl_2 \cdot 2H_2O$) was purchased from Alfa Aesar. Toluene anhydrous was purchased from Sigma-Aldrich Co. LLC.. All chemicals were used as received without further purification.

Synthesis of Al-MIL-101-NH_2

2-aminoterephthalic acid (1.09 g) and DMF (80 mL) were added into a round bottom flask. The solution was stirred at 110 ºC. $AlCl_3 \cdot 6H_2O$ (0.14 g) was added to the solution 7 times at 15 min intervals, while stirring at 110 ºC. After that, the mixture was stirred for 3 h, and placed in a static position at 110 ºC for 16 h. The obtained slurry was collected by centrifugation, washed with DMF and methanol several times and dried under vacuum overnight. The obtained light yellow powder was activated under vacuum at 160 ºC overnight.

The deamination of Al-MIL-101-NH_2

The deamination of Al-MIL-101-NH_2 was proceeded with a slight modification of the previous report (Fig. S1a).[1] Activated Al-MIL-101-NH_2 (100 mg) was put into a round bottom flask, which was sealed with a rubber septum. *t*-BuONO (1.0, 2.0, 4.0 mL) was added into the flask and stirred for 1 h at -20 ºC under Ar atmosphere. Anhydrous dichloromethane (8 mL) was added into the mixture with stirring at -20 ºC. The mixture was left without stirring at -20 ºC overnight. The product was collected by centrifugation and washed with methanol several times. The obtained product was dispersed in methanol (2 mL), and transferred Teflon lined stainless steel autoclave, and heated at 80 ºC for 3 h.

After cooling to room temperature, the mixture was centrifuged and washed with methanol and dichloromethane several times, and dried under vacuum overnight. The obtained product was named as Al-MIL-101-NH_2-X%, in which X represents the percentage of 2-aminoterephthalate contained in the deaminated sample determined from ^{1}H-NMR.

The linker exchange of Al-MIL-101-NH_2

The linker exchange of Al-MIL-101-NH_2 was proceeded with a slight modification of the previous report.[2] Activated Al-MIL-101-NH_2 (200 mg) and terephthalic acid (500 mg) was added into methanol (85 mL) in a round bottom flask and stirred for 48 h at 40 ºC. The product was collected by centrifugation and washed with methanol several times, and dried under vacuum overnight. The obtained product was named as Al-MIL-101-NH_2-X%, in which X represents the percentage of 2-aminoterephthalate contained in the deaminated sample determined from ^{1}H-NMR.

Synthesis of Al-MIL-53-NH_2

2-aminoterephthalic acid (0.54 g) and purified water (30 mL) were added into a round bottom flask. The solution was sonicated for 30 min. $AlCl_3 \cdot 6H_2O$ (0.72 g) was added to the solution with stirring. The mixture was sonicated for 30 min, transferred to Teflon lined stainless steel autoclave, and heated at 150 ºC for 6 h. The obtained product was collected by centrifugation, washed with DMF, purified water and methanol several times, and dried under vacuum overnight. The obtained yellow powder was activated under vacuum at 100 ºC for 6 h.

Synthesis of CAU-1

$AlCl_3 \cdot 6H_2O$ (2.97 g) and 2-aminoterephthalic acid (0.75 g) were added in methanol (30 mL). The mixture was sonicated for 15 min, transferred to Teflon lined stainless steel autoclave, and heated at 125 ºC for 5 h. The obtained product was centrifuged, washed with DMF, purified water and methanol several times, and dried under vacuum overnight. The obtained yellow powder was activated at 120 ºC overnight.

Synthesis of Cr-MIL-101-NH_2[3]

$Cr(NO_3)_3 \cdot 9H_2O$ (1.63 g), 2-nitroterephthalic acid (0.89 g), HF (0.16 g) and distilled water (20 mL) were stirred for 30 min. The mixture was transferred Teflon lined stainless steel autoclave, and heated at 220 ºC for 8 h. The obtained slurry was centrifuged, washed with purified water and acetone and dried under vacuum overnight. The obtained green Cr-MIL-101-NO_2 powder was activated at 160 ºC overnight.

As-synthesized Cr-MIL-101-NO_2 (0.20 g) and $SnCl_2 \cdot 2H_2O$ (1.40 g) were added into ethanol solution (60 mL) and stirred at 70 ºC for 6 h. Then, HCl (20 mL) was added into the mixture and stirred overnight. The mixture was centrifuged, washed with distilled water and acetone several times, and dried under vacuum overnight. The obtained yellow green powder was activated under vacuum at 160 ºC overnight. All of organic linkers of Cr-MIL-101-NO_2 was converted from 2-nitroterephthalate to 2-aminoterephthalate.

Synthesis of Fe-MIL-101-NH_2

Fe-MIL-101-NH_2 was synthesized by the same procedure of Al-MIL-101-NH_2, except for the metal precursor. The metal precursor changed from $AlCl_3 \cdot 6H_2O$ to $FeCl_3 \cdot 6H_2O$.

Characterization

Powder x-ray diffraction (XRD) patterns were obtained with a Rigaku Ultima IV diffractometer with Cu Kα radiation (λ = 1.5418 Å, 40 kV to 40 mA). UV-Vis diffuse reflectance spectra were collected on a Shimadzu UV-2600 spectrophotometer. The absorption spectra were obtained using the Kubelka-Munk function. Nitrogen (N_2) adsorption-desorption isotherm data was collected at -196 °C using a BELSORP-max system (MicrotracBEL Corp.). The specific surface area (S_{BET}) of the samples was calculated by a Brunauer–Emmett–Teller (BET) method. Fourier transform infrared (FT-IR) spectra were obtain with a JASCO FT/IR4100 spectroscopy. Proton nuclear magnetic resonance (^{1}H-NMR) spectra were obtained on a JEOL JNM-ECS 400 spectrometer operated at 400 MHz. Measurement sample solutions were prepared by dissolving MOF samples with 1 M NaOH in D_2O solution, followed by filtration. Ultraviolet photoelectron spectroscopy (UPS) measurements were carried out on a JEOL JPS-9010MX photoelectron spectrometer and a SPECS UVS10/35 Helium discharge tube, using a He I (21.22 eV) radiation light source. UPS measurements were performed with a voltage of -10 V. X-ray photoelectron spectroscopy (XPS) measurements were

conducted with a Shimadzu ESCA-3400 system. Mg Kα X-ray radiation (1253.6 eV) was used as the excitation source. The binding energy of Al 2p XPS spectra of Al-MOFs were calibrated with the adventitious carbon (C 1s) peak at 284.5 eV. Photoluminescence (PL) spectra were obtained using a Horiba Fluorolog-3 spectrofluorometer at room temperature. The excitation wavelength of PL measurements was 380 nm. Electron spin resonance (ESR) measurements were performed on a JEOL RESONANCE JES-TE200 spectrometer. For the ESR spectra of oxygen radicals in the reaction solution, the reaction solution contained DMPO (50 mM), which was dispersed Al-MIL-101-NH_2 (1.0 $g \cdot L^{-1}$), was added into an ESR tube and then subjected to analysis at room temperature under visible-light (λ > 420 nm) irradiation. Al-MIL-101-NH_2 was added into the mixed solution of acetonitrile and benzyl alcohol in the ESR tube by bubbling with pure O_2 for 30 min. The solution was frozen at -196 ºC after visible-light (λ > 420 nm) irradiation.

Photocatalytic H_2O_2 production

Photocatalyst (5.0 mg), acetonitrile (5.0 mL) and benzyl alcohol (1.0 mL) were added into a Pyrex reaction vessel (30 mL), which was sealed with a rubber septum. The mixture was sonicated and bubbled with oxygen for 15 min in dark. Thereafter, the reaction solution was irradiated from the side with an Xe lamp (500 W, 100 $mW \cdot cm^{-2}$, SAN-EIELECTRIC XEF-501S) through a glass filter (λ > 420 nm) for 4 h with magnetic stirring at ambient pressure and temperature.

H_2O_2 decomposition

MOF (5.0 mg) and acetonitrile (5.0 mL) contained 1.0 mM H_2O_2 were added in a Pyrex reaction vessel (30 mL), which was sealed with a rubber septum. The mixture solution was stirred under dark condition at ambient pressure and temperature for 3 h. The concentration of H_2O_2 decreased linearly with reaction time due to the decomposition reaction of H_2O_2 by MIL-101-NH_2 (**Fig. S10**). Therefore, the H_2O_2 decomposition rates of MOFs were calculated using the following equation:

$$H_2O_2\ decompostion\ rate\ = \frac{C_{H_2O_2,0h} - C_{H_2O_2,3h}}{3}$$

$C_{H_2O_2,0h}$: H_2O_2 concentration before the reaction, $C_{H_2O_2,3h}$: H_2O_2 concentration in 3 h.

Quantification of produced H_2O_2

The amount of produced H_2O_2 was determined from spectroscopic titration with an acidic solution of $[TiO(tpypH_4)]^{4+}$ complex (Ti-TPyP reagent). The $[TiO(tpypH_4)]^{4+}$ complex (3.4 mg) was dissolved in 50 mM HCl aqueous solution (100 mL). This solution was used as the Ti-TPyP reagent. The sample solution was diluted with water. The diluted sample solution (0.25 mL) was mixed with 4.8 M $HClO_4$ aqueous solution (0.25 mL) and Ti-TPyP reagent (0.25 mL). After a few minitues, the mixture was diluted to 2.5 mL with water. The absorbance of this solution at λ = 434 nm (A_S) was measured using a Shimadzu UV-2600 UV-Vis spectroscopy. A blank solution was prepared by adding water in place of the sample solution (0.25 mL) with its absorbance (A_B). The difference in absorbance (ΔA_{434}) was determined by the follow equation: $\Delta A_{434} = A_B - A_S$. Based on ΔA_{434} and volume of the solution, the amount of hydrogen peroxide was determined according to the literature.[4]

Quantification of produced benzaldehyde

The amount of produced benzaldehyde was quantified by gas chromatography (Shimadzu, GC-14B with Phenomenex ZB-FFAP columns)

Calculation of the number of photons emitted by a LED lamp

To calculate the apparent quantum yield (AQY) for Al-MIL-101-NH_2, the moles of photons emitted by the LED lamp were calculated by using the ferrioxalate actinometry method.[5] The method involves the reduction of potassium ferrioxalate in the presence of light, and the resulting Fe^{2+} ions are quantified by the complexation with 1,10-phenanthroline. Standard values for the quantum yield of Fe^{2+} formation can be utilized for the calculation of AQY of a specific photocatalytic reaction. The conditions for the preparation of solutions, and for the reaction (the formation of Fe^{2+}) were taken from the literature.[5] The moles of Fe^{2+} ($n_{Fe^{2+}}$) are calculated by using the latter equation:

$$n_{Fe^{2+}} = \frac{V_1 \cdot V_3 \cdot A}{10^3 \cdot V_2 \cdot L \cdot \epsilon}$$

V_1: irradiation volume (6.0 mL), V_2: sample taken (0.5 mL), V_3: final volume (5.0 mL), L: optical path-length (1.0 cm), A: absorbance difference at 510 nm (3.2589 at 400 nm irradiation), ϵ: absorbance coefficient (11100 L mol^{-1} cm^{-1}).

Then, the number of photons is calculated by using the formula below:

$$\frac{n_{photons}}{n_{min}} = \frac{n_{Fe^{2+}}}{\emptyset_{\lambda} \cdot t \cdot F}$$

$\emptyset_{\lambda}$: quantum yield for iron production at wavelength (1.14 at λ = 405 nm), t: time (2 min), F: mean fraction of light absorbed (1).

To calculate the AQY value, photocatalytic H_2O_2 production using Al-MIL-101-NH_2 was conducted in O_2-saturated acetonitrile solution with benzyl alcohol in 1 h of monochromatic light (λ = 405 nm) irradiation.

The AQY value is calculated based on the formula below:

$$\text{AQY (\%)} = 2 \cdot \frac{\frac{n_{H_2O_2}}{min}}{\frac{n_{photon}}{min}} \cdot 100$$

$n_{H_2O_2}$: the molar of H_2O_2 produced.

The calculation of the highest occupied crystal orbital (HOCO) of Al-MOFs

The highest occupied crystal orbital (HOCO) of the vacuum level standard was calculated based on the formula below:

$$HOCO_{vacuum} = 21.22 - \Delta E_{UPS}$$

$HOCO_{vacuum}$: HOCO of the vacuum level standard of Al-MOFs, ΔE_{UPS}: the width of the edges of the UPS spectrum.

The value of HOCO is exchanged from the vacuum level standard to the hydrogen electrode potential (NHE) standard by using the following equation:.

$$HOCO = HOCO_{vacuum} - 4.44$$

HOCO: HOCO of the NHE standard.

The lowest unoccupied crystal orbital (LUCO) of the SHE standard was calculated by the formula below:

$$LUCO = HOCO - E_g$$

LUCO: LUCO of the NHE standard, *Eg*: band gap energy calculated by the Tauc plot of the Al-MOF.

Density of state (DOS) calculations

To calculate the DOS for a series of MIL-101-NH_2, the plane wave-based program, Castep, was employed.[6,7] The Perdew, Burke, and Ernzerh (PBE) functional was used together with the ultrasoft-core potential model.[8] We employed slab models containing

three metal cations (Al, Cr, and Fe) and six coordinated 2-aminoterephthalic acid molecules confined within a 25 × 25 × 25 Å unit cell (**Fig. S8c-e**). All crystal structures were optimized within density functional theory (DFT) and H, N, C, and O atoms of these models allowed to relax during geometry optimizations. To properly describe the correlation energy of the strongly localized 3d orbital of the transition metals, the Hubbard U correction (DFT + U) was adopted using the method proposed by Dudarev et al.[9]

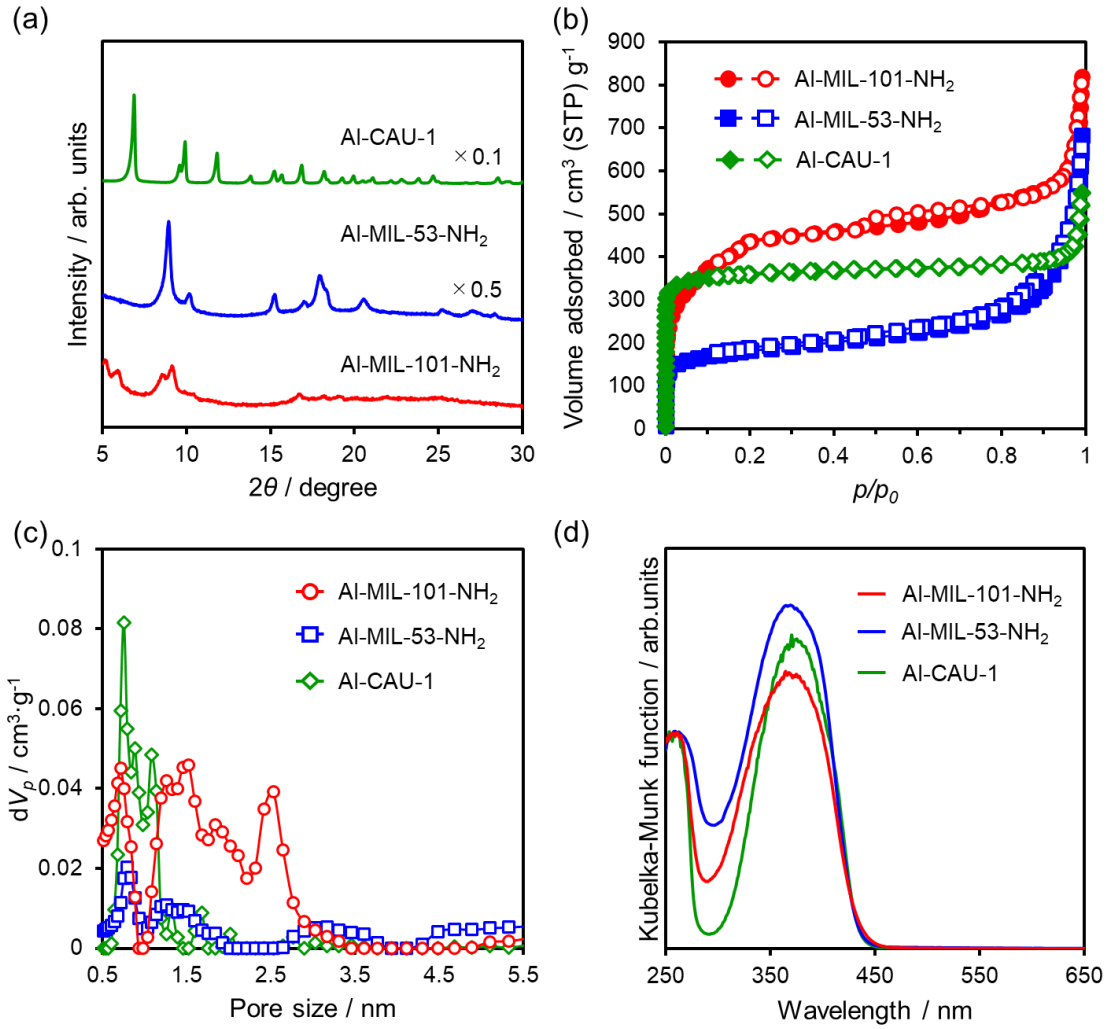

Fig. S1 (a) XRD patterns, (b) N_2 adsorption-desorption isotherms, (c) pore distributions estimated by the non–local density function theory (NLDFT) method, and (d) UV-Vis spectra of Al-MOFs.

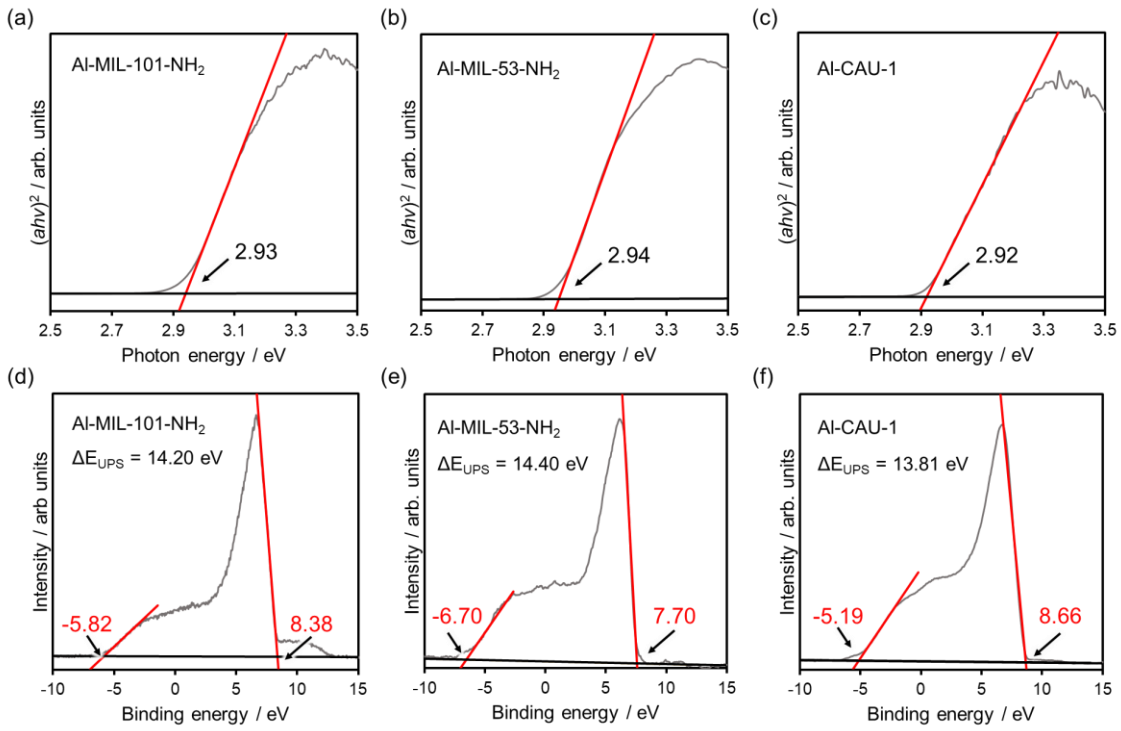

Fig. S2 The estimated band gap energies determined form the $(ahv)^2$ versus photon-energy plot of (a) Al-MIL-101-NH_2, (b) Al-MIL-53-NH_2, and (c) Al-CAU-1. UPS spectra of (d) Al-MIL-101-NH_2, (e) Al-MIL-53-NH_2, and (f) Al-CAU-1.

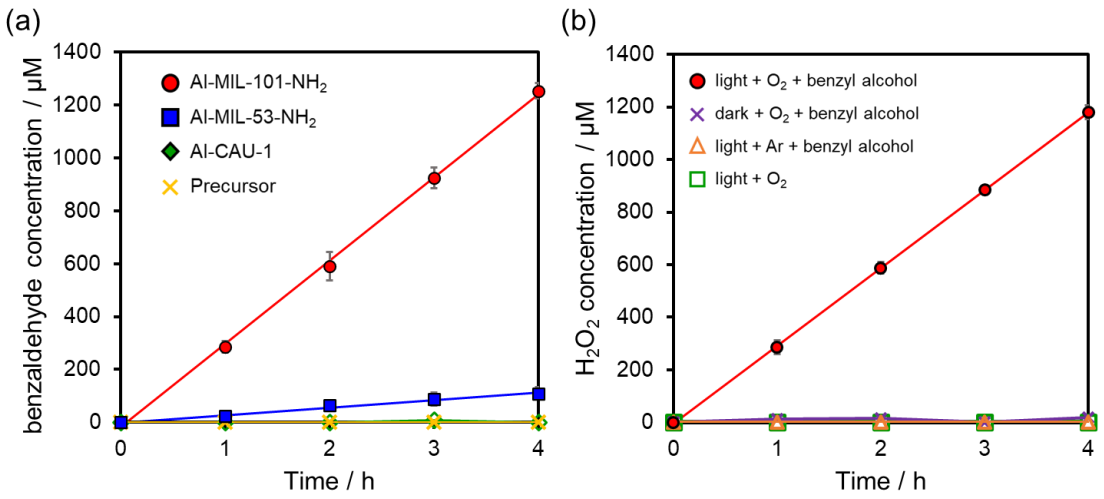

Fig. S3 (a) Time course of benzaldehyde production utilizing Al-MOFs in an O_2-saturated acetonitrile solution containing benzyl alcohol under visible-light ($\lambda > 420$ nm) irradiation. (b) Time course of H_2O_2 production utilizing Al-MOFs in various reaction conditions.

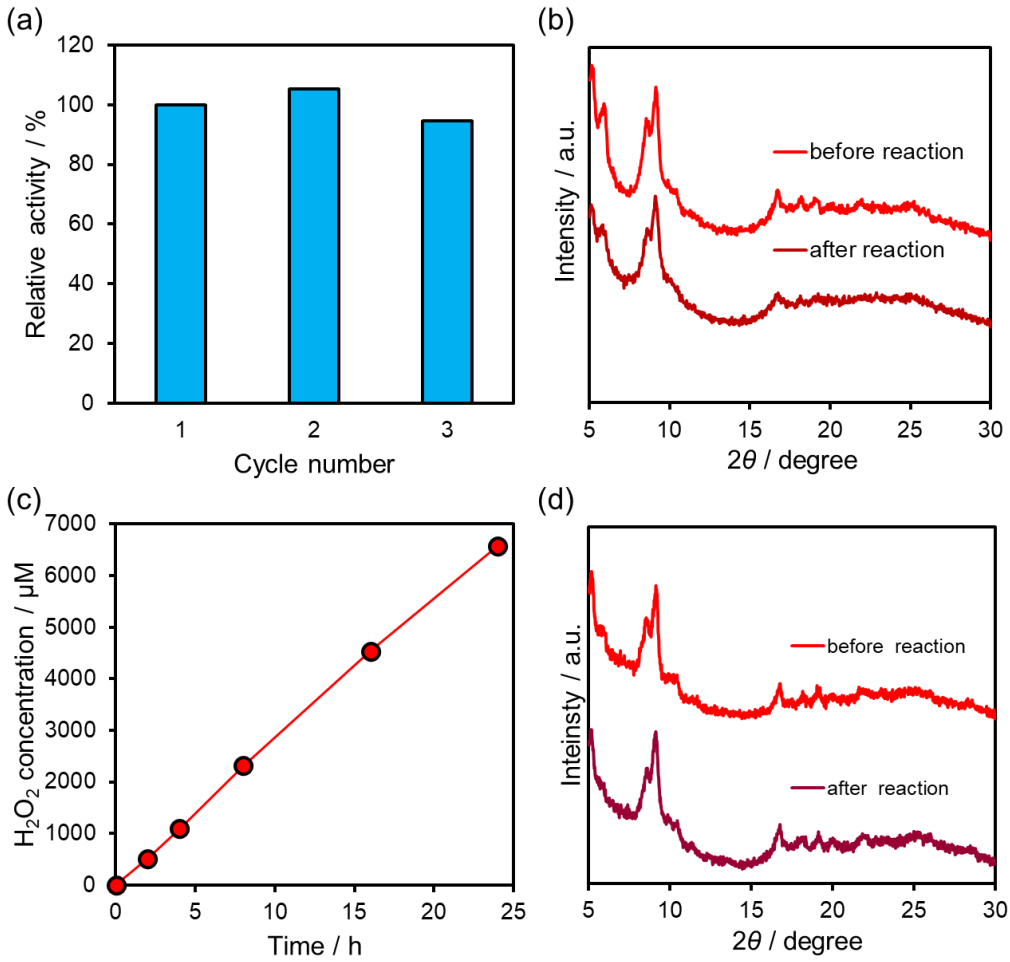

Fig. S4 (a) Recycling tests of Al-MIL-101-NH_2, (b) XRD patterns of Al-MIL-101-NH_2 before and after recycling tests. (c) Time courses of H_2O_2 production over Al-MIL-101-NH_2under visible-light ($\lambda > 420$ nm) irradiation during the long-term reaction. (d) XRD patterns of Al-MIL-101-NH_2 before and after the long-term reaction.

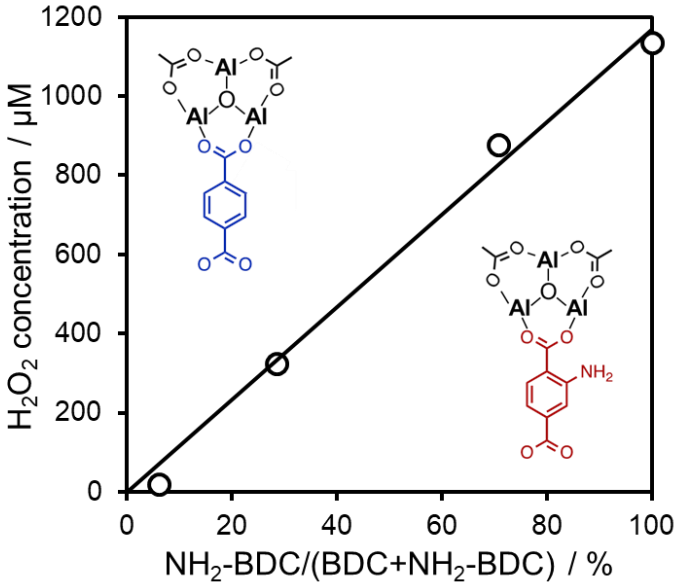

Fig. S5 The relationship between the concentration of H_2O_2 catalyzed by Al-MIL-101-NH_2-X% in 4.0 h of visible-light irradiation and the ratio of 2-aminoterephatalte (NH_2-BDC) to total organic linkers (NH_2-BDC + terephthalate (BDC)) in Al-MIL-101-NH_2.

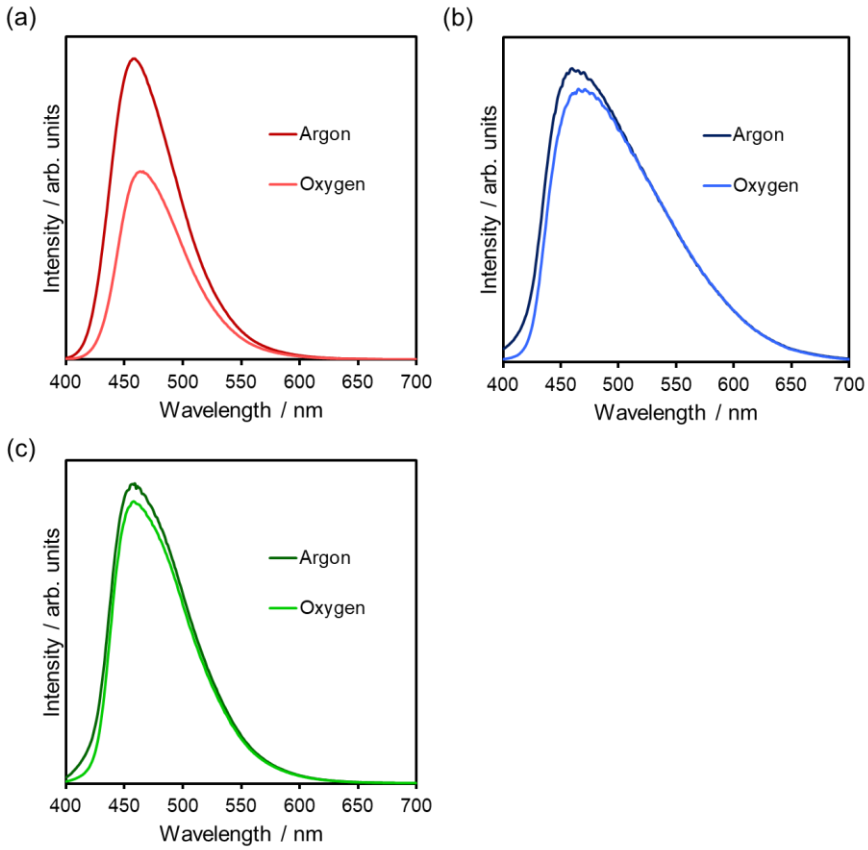

Fig. S6 Oxygen quenching on PL emission spectra of (a) Al-MIL-101-NH_2, (b) Al-MIL-53-NH_2, and (c) Al-CAU-1 measured under Ar atmosphere.

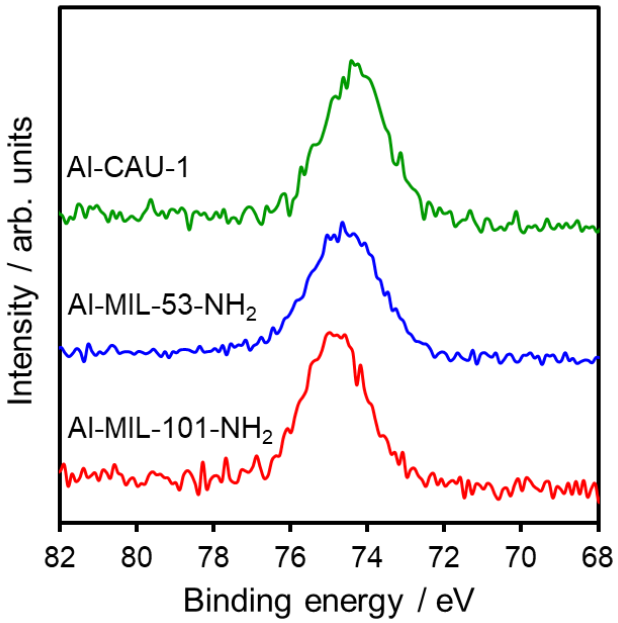

Fig. S7 Al 2p XPS spectra of Al-MOFs.

The peak of Al 2p of Al-MOFs sifted toward higher energy side in order to Al-MIL-101-NH_2 > Al-MIL-53-NH_2 > Al-CAU-1. In general, electron-deficient metal cations exhibit stronger Lewis acidity. These XPS results suggested that Al species of Al-MIL-101-NH_2 exhibited the strongest Lewis acidity in three Al-MOFs.

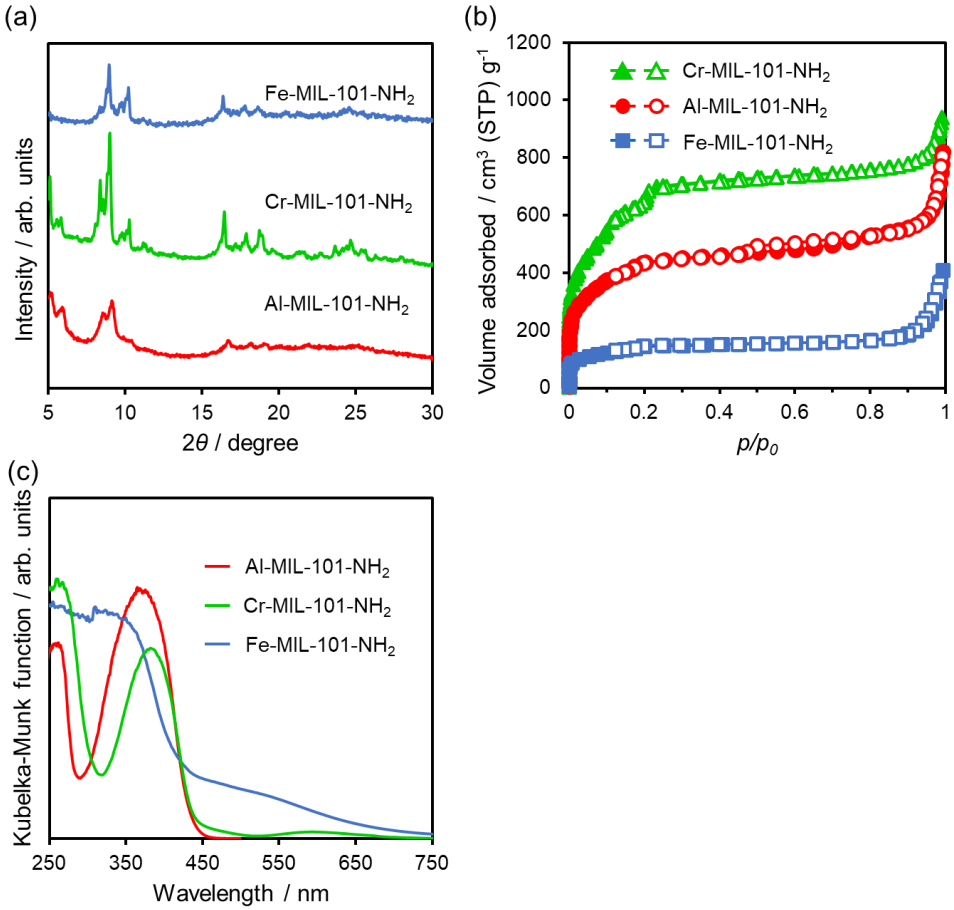

Fig. S8 (a) XRD patterns, (b) N_2 adsorption-desorption isotherms, and (c) UV-Vis diffuse spectra of MIL-101-NH_2.

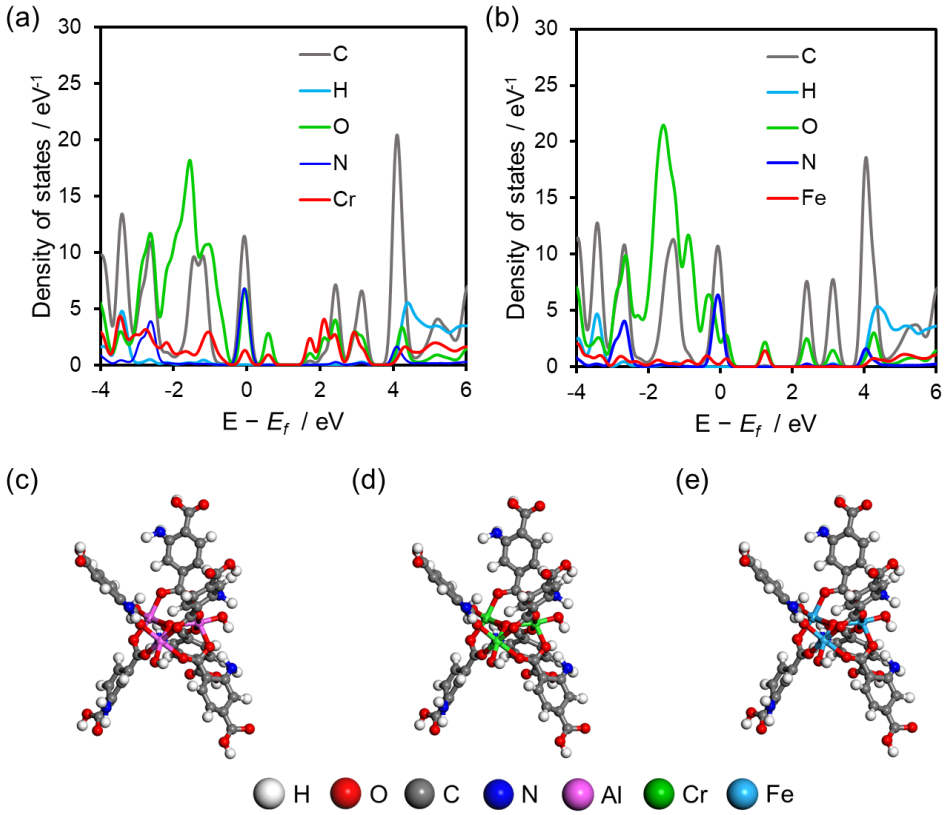

Fig. S9 Calculated DOS plots for (a) Cr-MIL-101-NH_2 and (b) Fe-MIL-101-NH_2. The models of (c) Al-, (d) Cr-, and (e) Fe-MIL-101-NH_2 for DOS calculation.

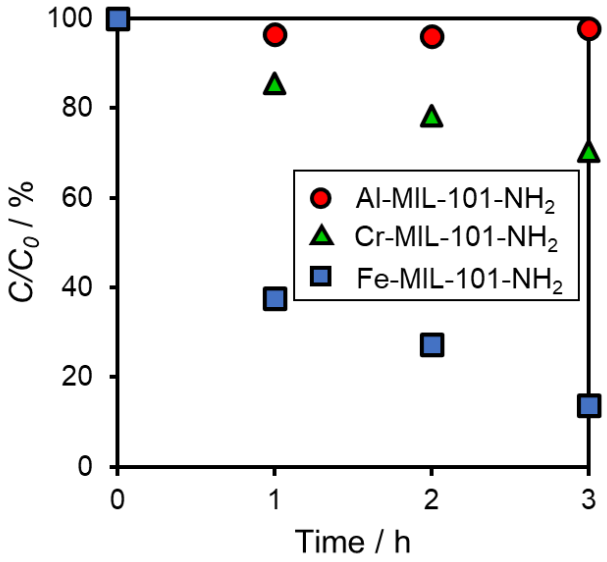

Fig. S10 Time course of a H_2O_2 decomposition tests using MIL-101-NH_2 in H_2O_2 contained acetonitrile solution at dark.

Table S1 N_2 adsorption data and optical properties of Al-MOFs.

Sample	S_{BET} / $m^2 \cdot g^{-1}$	V_p / $cm^3 \cdot g^{-1}$	E_g / eV
Al-MIL-101-NH_2	1580	1.23	2.93
Al-MIL-53-NH_2	664	1.00	2.94
Al-CAU-1	1421	0.81	2.92

Table S2 The value of ΔE_{UPS} and the energy levels of HOCO and LUCO of Al-MOFs.

Sample	ΔE_{UPS} / eV	*HOCO* / V vs NHE	*LUCO* / V vs NHE
Al-MIL-101-NH_2	14.20	2.58	-0.35
Al-MIL-53-NH_2	14.40	2.38	-0.40
Al-CAU-1	13.85	2.93	0.01

Table S3 The specific surface area and total pore volume of Cr-MIL-101-NH_2 and Fe-MIL-101-NH_2.

Sample	S_{BET} / $m^2 \cdot g^{-1}$	V_p / $cm^3 \cdot g^{-1}$
Cr-MIL-101-NH_2	2240	1.44
Fe-MIL-101-NH_2	490	0.62

Table S4 Comparison of H_2O_2 production in the presence of benzyl alcohol over photocatalysts.[10–12]

Entry	Catalyst	H_2O_2 production / μmol·h^{-1}·g^{-1}	H_2O_2 selectivity / %	Reaction condition	Irradiated light	reference
1	MIL-125-NH_2	52	5.7	Acetonitrile:benzyl alcohol (4:1)	Xe lamp, λ > 420 nm, 100 mW·cm^{-1}	10
2	MIL-125-0.14L2	246	4.1	Acetonitrile:benzyl alcohol (4:1)	Xe lamp, λ > 420 nm, 800 mW·cm^{-1}	11
3	UiO-66-NH_2-1.0	364	41.1	Acetonitrile:benzyl alcohol (4:1)	Xe lamp, λ > 350 nm, 100 mW·cm^{-1}	12
4	Al-MIL-101-NH_2	295	94.2	Acetonitrile:benzyl alcohol (4:1)	Xe lamp, λ > 420 nm, 100 mW·cm^{-1}	This work

References

1 A. Chołuj, N. I. Nikishkin and M. J. Chmielewski, *Chem. Commun.*, 2017, **53**, 10196–10199.

2 J. Marreiros, C. Caratelli, J. Hajek, A. Krajnc, G. Fleury, B. Bueken, D. E. De Vos, G. Mali, M. B. J. Roeffaers, V. Van Speybroeck and R. Ameloot, *Chem. Mater.*, 2019, **31**, 1359–1369.

3 S. Bernt, V. Guillerm, C. Serre and N. Stock, *Chem. Commun.*, 2011, **47**, 2838–2840.

4 C. Matsubara, N. Kawamoto and K. Takamura, *Analyst*, 1992, **117**, 1781–1784.

5 F. P. Kinik, A. Ortega-Guerrero, F. M. Ebrahim, C. P. Ireland, O. Kadioglu, A. Mace, M. Asgari and B. Smit, *ACS Appl. Mater. Interfaces*, 2021, **13**, 57118–57131.

6 M. C. Payne, M. P. Teter, D. C. Allan, T. A. Arias and J. D. Joannopoulos, *Rev. Mod. Phys.*, 1992, **64**, 1045–1097.

7 V. Milman, B. Winkler, J. A. White, C. J. Pickard, M. C. Payne, E. V Akhmatskaya and R. H. Nobes, *Int. J. Quantum Chem.*, 2000, **77**, 895–910.

8 D. Vanderbilt, *Phys. Rev. B*, 1990, **41**, 7892–7895.

9 S. L. Dudarev, G. A. Botton, S. Y. Savrasov, C. J. Humphreys and A. P. Sutton, *Phys. Rev. B*, 1998, **57**, 1505–1509.

10 Y. Isaka, Y. Kondo, Y. Kawase, Y. Kuwahara, K. Mori and H. Yamashita, *Chem. Commun.*, 2018, **54**, 9270–9273.

11 X. Chen, Y. Kuwahara, K. Mori, C. Louis and H. Yamashita, *J. Mater. Chem. A*, 2021, **9**, 2815–2821.

12 Y. Kondo, Y. Kuwahara, K. Mori and H. Yamashita, *J. Phys. Chem. C*, 2021, **125**, 27909–27918.